Cell Motility and the Cytoskeleton (2006)

Sensitivity of Alveolar Macrophages to Substrate Mechanical and Adhesive Properties

Sophie Féréol, Redouane Fodil, Béatrice Labat, Stéphane Galiacy, Valérie M. Laurent, Bruno Louis, Daniel Isabey,* and Emmanuelle Planus

Inserm UMR 651, Fonctions Cellulaires et Moléculaires de l'Appareil Respiratoire et des Vaisseaux, Equipe Biomécanique Cellulaire et Respiratoire et Université Paris XII, Faculté de Médecine, Institut Supérieur des Biosciences de Paris, Créteil, France

In order to understand the sensitivity of alveolar macrophages (AMs) to substrate properties, we have developed a new model of macrophages cultured on substrates of increasing Young's modulus: (i) a monolayer of alveolar epithelial cells representing the supple (∼0.1 kPa) physiological substrate, (ii) polyacrylamide gels with two concentrations of bis-acrylamide representing low and high intermediate stiffness (respectively 40 kPa and 160 kPa) and, (iii) a highly rigid surface of plastic or glass (respectively 3 MPa and 70 MPa), the two latter being or not functionalized with type I-collagen. The macrophage response was studied through their shape (characterized by 3D-reconstructions of F-actin structure) and their cytoskeletal stiffness (estimated by transient twisting of magnetic RGD-coated beads and corrected for actual bead immersion). Macrophage shape dramatically changed from rounded to flattened as substrate stiffness increased from soft ((i) and (ii)) to rigid (iii) substrates, indicating a net sensitivity of alveolar macrophages to substrate stiffness but without generating F-actin stress fibers. Macrophage stiffness was also increased by large substrate stiffness increase but this increase was not due to an increase in internal tension assessed by the negligible effect of a F-actin depolymerizing drug (cytochalasine D) on bead twisting. The mechanical sensitivity of AMs could be partly explained by an idealized numerical model describing how low cell height enhances the substrate-stiffness-dependence of the apparent (measured) AM stiffness. Altogether, these results suggest that macrophages are able to probe their physical environment but the mechanosensitive mechanism behind appears quite different from tissue cells, since it occurs at no significant cell-scale prestress, shape changes through minimal actin remodeling and finally an AMs stiffness not affected by the loss in F-actin integrity. Cell Motil. Cytoskeleton 2006.

Key words: alveolar epithelial cells; cell/substrate stiffness; F-actin; magnetic twisting cytometry; mechanotransduction; prestress

INTRODUCTION

Pulmonary alveoli are lined by epithelium, composed of several cell types, such as type II alveolar epithelial cells, on which Alveolar Macrophages (AMs) spread, adhere and migrate. AMs are the principal resident free cells of the distal airspaces and are responsible for maintaining a bacteria and particle free environment

*Correspondence to: Daniel Isabey, Inserm UMR 651, Faculté de Médecine - 8, rue du Général Sarrail, 94010 Créteil Cedex, France. E-mail: daniel.isabey@creteil.inserm.fr

Received 15 November 2005; Accepted 28 February 2006

Published online in Wiley InterScience (www.interscience.wiley.com). DOI: 10.1002/cm.20130

in the lower respiratory tract. AMs are highly motile cells and their ability to migrate towards a source of chemoattractant is essential for their recruitment to sites of inflammation. In spite of the fact that the fundamental role of AMs involves its interactions with neighboring cells, large gaps remain in our knowledge of how AM respond to an alveolar environment which is susceptible to deep changes. In normal physiological conditions, pulmonary macrophages are entirely covered by a surface lining layer which indeed regulates surface tension. It has been reported that bronchiolar macrophages can bulge into the airspaces for normal or low surface tension, while in the case of high surface tension associated to reduced surface curvatures (e.g., surfactant depletion), bronchiolar macrophages are molded like pancakes onto the epithelial surfaces [Bachofen and Schurch, 2001]. During acute lung injury, the alveolar-capillary barrier is subjected to considerable stretching during breathing and mechanical ventilation [Tschumperlin and Margulies, 1999]. At the same time, inflammatory mediators - dependent on AMs stretching [Pugin et al., 1998] - tend to compromise the alveolar epithelium integrity through deep modifications of the force balance at the cell-cell junction. Recent results show that both stretching and inflammation enhance epithelial cell stiffness and alteration of the alveolo-epithelial barrier integrity [Trepat et al., 2004; Trepat et al., 2005], thus rendering stiffer and more heterogeneous the AMs susbtrate in the injured epithelium.

Changes in cell shape are known to be mediated by alterations in the cytoskeleton (CSK), and the substrate appears to control cell shape and function by producing global changes in a structurally integrated CSK network [Folkman and Moscona, 1978; Bissell and Barcellos-Hoff, 1987; Ben-Ze'ev et al., 1988; Mooney et al., 1995]. Such substrate-dependent CSK changes occur because cell membrane adhesive structures constitute potential site at which acto-myosin contractile CSK forces are exerted on the substrate [Miyamoto et al., 1995; Chrzanowska-Wodnicka and Burridge, 1996; Beningo et al., 2001]. These concepts have been particularly well established for tissue cells as pointed out in a recent review by Discher et al. [Discher et al., 2005]. The contractile forces generated in the CSK by the actin-myosin motors are known to be counter-balanced by the anchoring forces exerted through the molecular interactions (e.g., cluster of integrins) at the adhesion sites on the substrate [Balaban et al., 2001]. Moreover, it has been shown that the strength of integrin-cytoskeleton linkages is dependent on matrix rigidity and its biochemical composition [Choquet et al., 1997; Sheetz et al., 1998]. Cell movement can also be guided by purely physical interactions at the cell-substrate interface and this apparent preference for a stiff substrate is called "durotaxis" [Lo et al., 2000]. Moreover, cells adherent to flexible substrates showed reduced spreading and increasing rates of motility or lamellipodial activity compared to rigid substrates [Pelham and Wang, 1997].

By contrast, macrophage response to substrate stiffness remains largely unknown. To our knowledge, it has been shown that AM phagocytosis, a process which corresponds to a form of cell movement, Beningo and Wang found that when presented with particles with identical chemical properties but different stiffness, AMs showed a strong preference to engulf stiff objects [Beningo and Wang, 2002]. In order to assess AM sensitivity to various substrate mechanical properties, we compared, in the same culture conditions but for a variety of substrates: i) the shape of AMs assessed from 3D-reconstructions of the F-actin network of adherent rat AMs, and ii) the measured elasticity modulus of living rat AMs. Properties of tested substrates ranged from supple to rigid, namely : (i) a physiological cellular substrate consisting of an alveolar epithelial cell monolayer, (ii) two flexible synthetic substrates (soft and stiff) of intermediate stiffness composed of polyacrylamide gels, and (iii) a rigid substrate (plastic or glass) coated or non coated with type I collagen. Measurements of cell elasticity modulus (called AMs stiffness) were performed using an improved Magnetic Twisting Cytometry device (MTC) based on bead rotation measurement beyond torques of 400 pN$\times$µm and our approach of the correction for actual bead immersion within the cytoplasm [Laurent et al. 2002b; Fodil et al., 2003; Ohayon et al., 2004]. In parallel, change in AMs shape was studied for the different tested substrates on the basis of 3D-reconstructions based on the Z-stack of optical sections obtained by confocal microscopy. This structural study reveals that AMs are sensitive to large substrate stiffness alterations. Moreover, AMs stiffness was altered by changes in substrate stiffness while cell stiffness was surprisingly not affected by F-actin depolymerization. It appears from results presently obtained that behavior of AMs differs from tissue cells, e.g., smooth muscle cells and endothelial cells [Wang et al., 1993, 2002; Hu et al., 2004, 2005], fibroblasts [Bausch et al., 1998; Dembo and Wang, 1999; Munevar et al., 2001], myocytes [Griffin et al., 2004], in all of which cell prestress was found to be central for mechanosensing and cell adaptation to the mechanical environment. Noteworthy, present results suggest that low tensed mechanotransduction pathways could exist in AMs, which might explained their peculiar substrate sensitivity.

MATERIALS AND METHODS

Materials

RGD peptide was obtained from Telios Pharmaceuticals Inc. (San Diego, CA, USA), mounting medium

was obtained from DAKO (Carpinteria, CA, USA). Carboxyl Ferro-Magnetic beads (#CFM-40-10) were purchased from Spherotech Inc. (Brussels, Belgium). Trypsin, EDTA, Foetal Calf Serum (FCS), Penicillin, Streptomycin, Bovine Serum Albumin (BSA), Cytochalasin D, rhodamine phalloidin were purchased from Sigma Chemicals (l'Ile d'Abeau Chêne, France). DMEM containing glutamax, 4500 mg/l D-glucose, sodium pyruvate and RPMI 1640 were purchased from Invitrogen (Eragny sur Oise, France). Type I collagen and adhesion molecule antibodies were purchased from BD Biosciences (Pont de Claix, France).

Cell Isolation and Culture

Isolation of Alveolar Epithelial Type II Cells. Alveolar type II cells were isolated from pathogen-free male Sprague-Dawley rats as previously described [Clerici et al., 1992; Planus et al., 1999]. Culture medium was DMEM containing 10% FCS, 50 IU/ml penicillin, 50 μg/ml streptomycin. Plated cells were incubated in a 5% CO_2–95% air incubator. After 24 h, the culture medium was changed for a medium composed of DMEM supplemented with 50 IU/ml penicillin, 50 μg/ml streptomycin, and 0.1% BSA. Confluence was reached within 5 days.

Isolation of Alveolar Macrophages. AMs were isolated from pathogen-free male or female Sprague-Dawley rats weightings 375–400 g (IFFA CREDO). Animals were injected with 30 mg/kg i.p. pentobarbital sodium. After exsanguination, the trachea was cannulated and bronchoalveolar lavages were performed with 100 ml of Solution I containing 140 mM NaCl, 5 mM KCl, 2.5 mM PBS, 10 mM Hepes, 6 mM D-glucose and 0.2 mM ethylene diamine tetraacetic acid tetrasodium salt (EDTA) at 37°C. The heterogeneity in cell shape and function, which is inherent to an AM population issued from bronchoalveolar lavage, has been minimized as proposed by Laplante et al. [Laplante and Lemaire, 1990] by choosing to study AMs isolated from the second fraction of broncho-alveolar lavage fluid, these AMs were recognized to have a better adherence and most likely a better homogeneity.

Lavage fluids were centrifuged at 500 g for 10 min and the cells pellet was re-suspended in RPMI medium supplemented with 0.1% BSA. An average yield of 4×10^6 cells/rat was obtained. The time allowed for AM adhesion (i.e., ~3 hours) was chosen as a compromise between optimal adhesion and minimal de-differentiation [Rossman et al., 1980]. For each set of substrates studied, (i.e., epithelial cells, gels, glass/plastic), the macrophages pertaining to the same population, (i.e., issued from the same rat) were seeded in culture wells without addition of any chemoattractant.

Cell Adhesion Assay

Cell adhesion assay were performed to determine the nature of the integrins involved in the adhesion of AMs for various substrates. After isolation of rat AMs, cells in suspension were pre-incubated under gentle agitation for 30 min at 4°C with 10 mg/ml of either (i) anti-CD18 mAb monoclonal antibody (mAb), or (ii), anti-CD11b, or (iii) both anti-CD18 and anti-CD11b mAb. Following pre-incubation, AMs were seeded at a density of 1.5×10^6cells/ml onto two types of tested substrates, namely the cellular and the rigid plastic substrates (coated and non-coated with type I collagen) and incubated for 3 h. Non-adherent cells were then removed by three rinses with warm PBS (37°C). Adherent cells were fixed with 1% glutaraldehyde in PBS for 30 min, and then rinsed three times with PBS. Lastly, cells were covered by DAKO mounting medium. The number of adherent AMs on the various substrates was evaluated after 3 hours of seeding, from 10 photos obtained by phase contrast microscopy with ×20 objective.

Staining of F-Actin With Fluorescent Phallotoxin

Rat type II pneumocytes were isolated as described above and then plated at a density of 10^6 cells per cm^2 on Lab-Tek chambered coverglass (8 wells) previously coated with type I collagen. Five days later, rat type II pneumocytes had formed a confluent cell monolayer and AMs isolated by bronchoalveolar lavages were seeded over the monolayer for 3 h before fixation and staining. Staining of F-actin was carried out as previously described [Doornaert et al., 2003]. Briefly, after fixation of the co-culture with 1% glutaraldehyde and then staining with rhodamine phalloidin (1.5 μM), cells were covered with mounting medium and stored at 4°C overnight before observation by laser confocal microscopy.

Confocal Microscopy and 3D-Reconstructions of F-Actin Structure

Confocal microscopy and 3D-reconstructions of F-actin structure were performed as previously described [Laurent et al. 2002b; Fodil et al., 2003]. Fluorescent stained AMs were observed using the LSM 410 invert confocal microscope (Zeiss, Rueil-Malmaison, France) and were brought into focus using a ×100/1.3 numeric aperture Plan-Neofluar objective. Optical sections were recorded every 0.3 μm to reveal intracellular fluorescence. Visualization of CSK-actin was performed using 3D-Studio Max v6.0 software (Kinetix, CA USA) and was supposed to represent the submembranous F-actin structure

Magnetic Twisting Cytometry to Measure Elasticity Modulus of AMs

Cell elasticity modulus was assessed by a previously described laboratory-made Magnetic Twisting Cytometry device (MTC) [Planus et al., 1999; Wendling et al., 2000; Laurent et al. 2002b] similar to that initially described by Wang et al. [Wang et al., 1993], i.e., an MTC method based on the measure of mean rotation of twisted ferromagnetic RGD-coated beads. The difference with initial MTC method is that the torque-bead rotation relationships used to deduce the actual cell stiffness from the apparent cell stiffness (or torque divided by the product: bead rotation×bead volume) is corrected by a factor deduced from a theoretical model which takes into account the physics of bead immersion [Laurent et al. 2002b; Ohayon et al., 2004; Ohayon and Tracqui, 2005]; the half-angle of bead immersion being measured from 3D-reconstructions of the AM F-actin structure following a method previously described (see [Fodil et al., 2003 #139] Fig. 6 of section Results). In the studied AMs, after 30 min of incubation, typical values of half-angle of bead immersion in AMs were found to be $108^\circ \pm 30^\circ$ estimated for a population of 10 beads (see Results). In the present study, the torque applied to the beads was maintained constant and equal to 800 pN × μm (corresponding to a 5 mT perpendicular magnetic field) but we preliminary verified that AM elasticity modulus was actually not affected by values of applied magnetic torques varying in the range 400–1000 pN × μm. The average bead rotation angle was measured by an on-line magnetometer over the entire bead/cell population present in the culture.

AM Culture for MTC Measurements

Rat AMs were plated at a density of 10^6 cells/ml (i) in bacteriological dishes (96-well) coated or not with type I collagen, or (ii) covered by a confluent monolayer of rat pneumocytes seeded 5 days sooner in similar bacteriological dishes basically coated with type I collagen. AMs were allowed to adhere and spread in RPMI 1640 medium supplemented with 0.1% BSA for 3 h, before performing an MTC experiment. Before use, AMs were incubated in RPMI 1640 medium supplemented with 1% BSA for at least 30 min at 37°C to block non-specific binding. RGD-coated ferromagnetic beads were then added to the cells (40 μg per well) for 30 min at 37°C in a 5% CO_2–95% air incubator. Unbound beads and AMs were washed away systematically three times with RPMI 1640 medium supplemented with 1% BSA. We verified in a previous study that neither three repeated rinsing nor bead twisting significantly affected the remnant magnetic field or the stiffness measurement [Ohayon et al., 2004].

To study the effect of actin depolymerization on the mechanical properties of AMs plated on different substrates, we used treatments with low concentrations of cytochalasin D (1 μg/ml) for 11 min before MTC measurements.

Preparation of Polyacrylamide Gels

Polyacrylamide gels were prepared according to a method previously described by Wang et al. [Wang and Pelham, 1998]. Briefly, thin sheets of polyacrylamide gel were prepared from a misture of 10% acrylamide and 0.07% (or 0.3%) *N*,*N*-methylene-bis-acrylamide. Ten microlitres of this mixture were placed onto the surface of a circular coverslip (30 mm diam.) and covered with small circular activated coverslip (12 mm diam.). After polymerization, the large coverslips on which polyacrylamide gels were polymerized, were removed and the gels were rinsed with 100 mM Hepes. To covalently attach type I collagen onto surface of the polyacrylamide gel, we used the photoactivatable heterobifunctional reagent sulfosuccinimidyl 6 (4-azido-2-nitrophenyl-amino) hexanoate (sulfo-SANPAH). After photoactivation, a 0.2 mg/ml solution of type I collagen was layered onto the substrate and allowed to react overnight at 4°C. The gels were stored at 4°C. Before plating cells, gels were soaked for 30–45 min in culture medium at 37°C. Performing indentation with an atomic force microscope, Nanowizard (JPK Instruments, Berlin, Germany), we verified that elasticity modulus of gels was close to predicted values by the literature [Engler et al., 2004; Yeung et al., 2005], i.e., 40 kPa for 0.07% of bis-acrylamide and 160 kPa for 0.3%.

Collagen Coating

Concentrated stocks of type I rat tail collagen (BD Biosciences) were diluted in 0.02 N glacial acetic acid to 5μg/cm^2. The diluted proteins were dispensed into bacteriologic dishes (96-well) (100μl/well) and into Lab-Tek chambered coverglass (8 wells) (200 μl/well) and incubated for 3 hours at room temperature. Coated wells were routinely washed 3 times with sterile water, dried and kept at 4°C.

Numerical Model of the Macrophage–Substrate Mechanical Interaction

To specifically study the contribution of substrate mechanical properties to the AM stiffness measured by partially embedded rotating beads, we modified a previously published finite element model. This model described the bead-cell monolayer mechanical interactions [Ohayon et al., 2004], by substituting isolated rectangular blocks - representing isolated AM - for the uniform cell monolayer representing confluent epithelial cells. Each block had a surface, height and elasticity properties representative of a given AMs. The half-angle of bead immersion in each block was in the range $\alpha = 100^\circ$–130° for a bead-radius of around 2.25 μm. Sub-

strate monolayer was defined by its elasticity properties covering the ranges of tested Young modulus and mean cell height. Defining a representative substrate volume element by $3a \times 3a \times h_s$ (h_s: mean height of the substrate), the representative volume element of AM was taken to be $2a \times 2a \times h_m$ (h_m: mean height of the AM). Note that a macrophage/substrate length ratio of 2/3 leads to a realistic volume ratio between the simulated AM and the representative substrate element. The value of "a" was taken to be 9 μm, which corresponds to an overall AM area of 324 μm^2, approaching the maximal AM area found on glass substrates (see Fig. 6A). The height of the macrophage was taken in the range (h_m: 5–11 μm) thus including the values found in AMs from flattened (h_m: 5 μm) to rounded (h_m: 8 μm). We assumed no-slip boundary conditions at the bead-cell interface and at the AM-substrate interface. Zero displacement condition, meaning full attachment of the substrate to a non-deformable base was also assumed. Other boundaries remained free. Preliminary experiments have shown that AMs exhibit a linear elastic behavior, i.e., a linear torque-bead rotation relationship, thus justifying the linearity assumption used in the present model. Simulations were performed under static conditions assuming incompressible medium. A finite element approach previously described in [Ohayon et al., 2004; Ohayon and Tracqui, 2005] was used to compute the substrate-dependent Young modulus, E_{app}, seen by the bead, comparatively to an assumed Young modulus of the cell, E_{cell}.

RESULTS

Characterization of the Physiological Substrate Used for AM Adhesion

To study shape and mechanical properties of AMs in their physiological environment, we developed a co-culture model presented in Fig. 1A in which isolated rat AMs can adhere, spread and migrate on a cellular substrate made of a monolayer of alveolar epithelial cells polarized in the apico-basal direction. After healthy differentiation, type II cells form a cell monolayer characterized by a complete confluence with tight intercellular junctions (Fig. 1A). When the same AMs are cultured on glass substrate (Fig. 1B), AMs modify their shape, a phenomena which is quantitatively analyzed in paragraphs below in order to characterize the AM sensitivity to substrate.

It should be noted first that the mechanical characterization by RGD-coated beads of an epithelial monolayer of type II cells was found not possible, most likely because these 5-days culture acquire a strong apico-baso-lateral polarity with tight junctions. This polarity presumably induces a redistribution of integrins receptors towards the basal location, impeding RGD coated beads to physically access at the apical face through integrin receptors. This was ascertained by the absence of detectable resident magnetic field after the application, on these cells, of the standard bead attachment procedure (see Materials and Methods). It means that contrary to what normally occurs over monolayer of alveolar epithelial cell lines (A549), the RGD coated beads could not interact with epithelial monolayer of type II cells. This can be verified on the microscopic image shown in Fig. 1C. When alveolar epithelial cells are at confluence and tightly connected, i.e., they get their apico-baso-lateral polarity, they cannot bind any beads; by contrast, when these cells "dedifferentiate" and then get a front-rear polarity to be able to migrate in the wound, they are again able to bind RGD-coated beads.

Taking advantage of this specificity of the primary culture of alveolar epithelial type II cells, we were able to measure the mechanical properties of AMs co-cultured, i.e., adherent, over the epithelial monolayer because AMs do bind the RGD coated beads (Fig. 1D) while the underlying type II alveolar cells did not. Opportunely, the defect in bead attachment specifically found in type II alveolar cells rendered possible the use of the MTC method in co-culture, allowing to specifically measure elasticity modulus of AMs while they adhere on a physiological substrate. Nevertheless, a residual problem for the present study is the mechanical characterization of the type II cellular monolayer substrate which remained impossible by MTC. To characterize the epithelial cell substrate, we then used the value of elasticity modulus measured by MTC method in the A549 human epithelial cell lines, i.e., 0.1 kPa, obtained after appropriate correction for the actual bead immersion angle, i.e., $\alpha = 67^\circ$ in these cells [Laurent et al. 2002b; Ohayon et al., 2004; Ohayon and Tracqui, 2005].

Characterization of Alveolar Macrophage Adhesion

Adhesion experiments in which AMs were pre-incubated with 10 mg/ml anti-CD18 mAb for 30 min (see Materials and Methods) were performed in order to determine the proportion the integrin subunit β_2 (CD18) involved in the interactions between AMs and two types of tested substrates, namely the cellular and the rigid plastic substrates (coated and non-coated with type I collagen). The results presented in Fig. 2, show that pre-treatment of AMs with antibodies directed against the integrin subunit β_2 (CD18), significantly reduced adhesion whatever the type of tested substrate. Compared to non-treated AMs, anti-CD18 mAb blocked adhesion to rigid non-coated plastic 69% (±17.5), adhesion to type I collagen-coated plastic by 92% (±3) and adhesion to

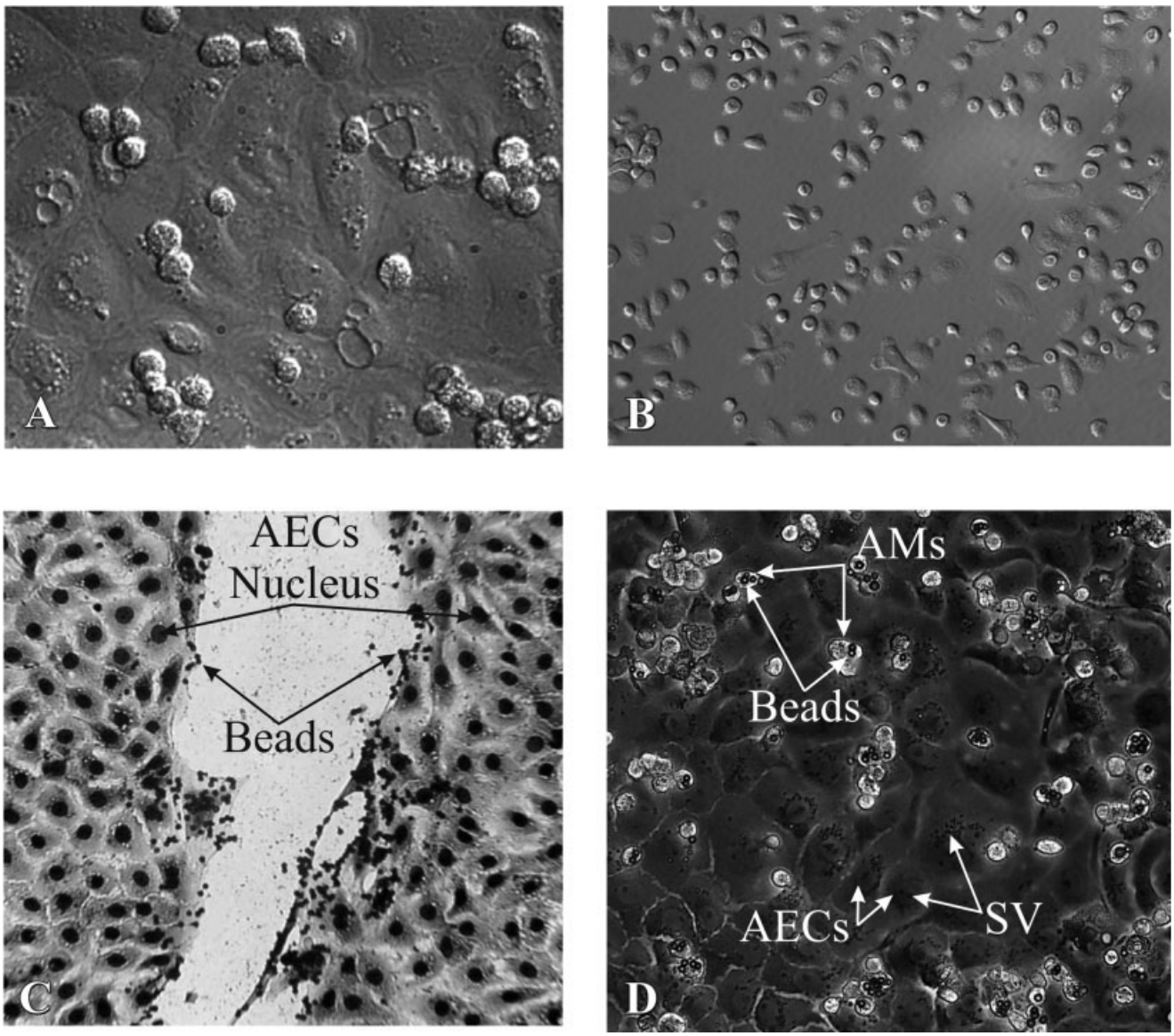

Fig. 1. A and B provide views of isolated rat alveolar macrophage population on two different substrates: (in A) on type II alveolar epithelial cell monolayer (objective: ×40), (in B) on glass substrate (objective: ×20). Views A and B show qualitatively that differences in AM shapes observed when the substrate properties changes (i.e., rounded on cell substrate and flattened on rigid substrate). Note that, in our culture conditions, the wide majority of AMs exhibit a symmetrical shape whether there are rounded or flattened while front-rear polarity shape concern a limited number of AMs. C provides views of RGD-coated bound bead distribution on type II alveolar epithelial cell (AECs) monolayer fixed and stained by Giemsa and in which a wound is created mechanically by a micropipette tip. At a distance from the wound edge, AECs are at confluence and tightly connected and cannot bind any beads likely due to the lack of integrin expression at their apical surfaces. The stained nucleus of AECs are dark. By contrast, when these cells "dedifferentiate" and then get a front-rear polarity to be able to migrate in the wound, they become able to bind RGD-coated beads which is clearly shown on the image in C. D shows (objective: ×20) the RGD-coated bead distribution in case of AMs cultured on a confluent type II AEC monolayer. RGD-coated bound beads are only visible on AMs and not at all on type II AECs. AECs exhibit secretary vesicules (SV) visible on their upper face in D and even in A.

cellular monolayer by 75% (±10). Since according to Ross et al. and Albert et al. [Albert et al., 1992; Ross, 2000], α_M/β_2-integrin is the only integrin which interacts with collagen, plastic substrate, as well the ICAM-1 receptor of type II alveolar epithelial cells, we also inhibited the integrin subunit α_M (CD11b). This did not have any significant effect on AM adhesion for the two types of substrate tested. Similarly, we did not observed a synergistic effect on AM adhesion when both anti-CD11b and anti-CD18 mAb were directed against CD11b and CD18 integrins. These results show that integrin subunit β_2 (CD18) is implicated in AM adhesion.

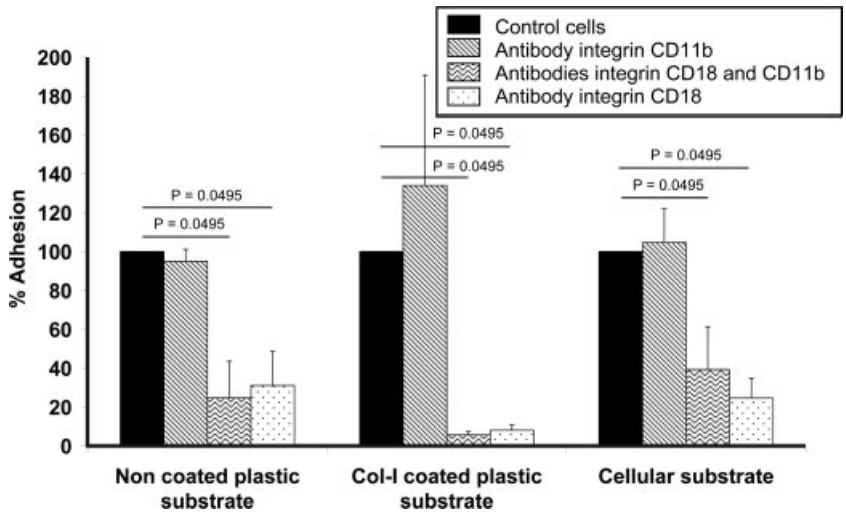

Fig. 2. Control adhesion experiments. AMs were pre-incubated with 10 mg/ml of (1) antibody against integrin CD11b, (2) antibody against integrin CD18, (3) both antibodies against CD11b and CD18. Following pre-incubation, the cells were seeded onto three different surfaces: (1) plastic substrate, (2) type I collagen coated plastic substrate and (3) cellular substrate incubated for 3 hours. Non-adherent cells were then removed by three washes. Treatment of AMs with antibody direct against integrin CD18 substantially blocked AMs adhesion to the three substrates, indicating that integrin CD18 is necessary for attachment to these various substrates. Values are mean ± s.e.m. Each value is the mean of three independent measurements. The statistical test used was the Mann–Whitney test.

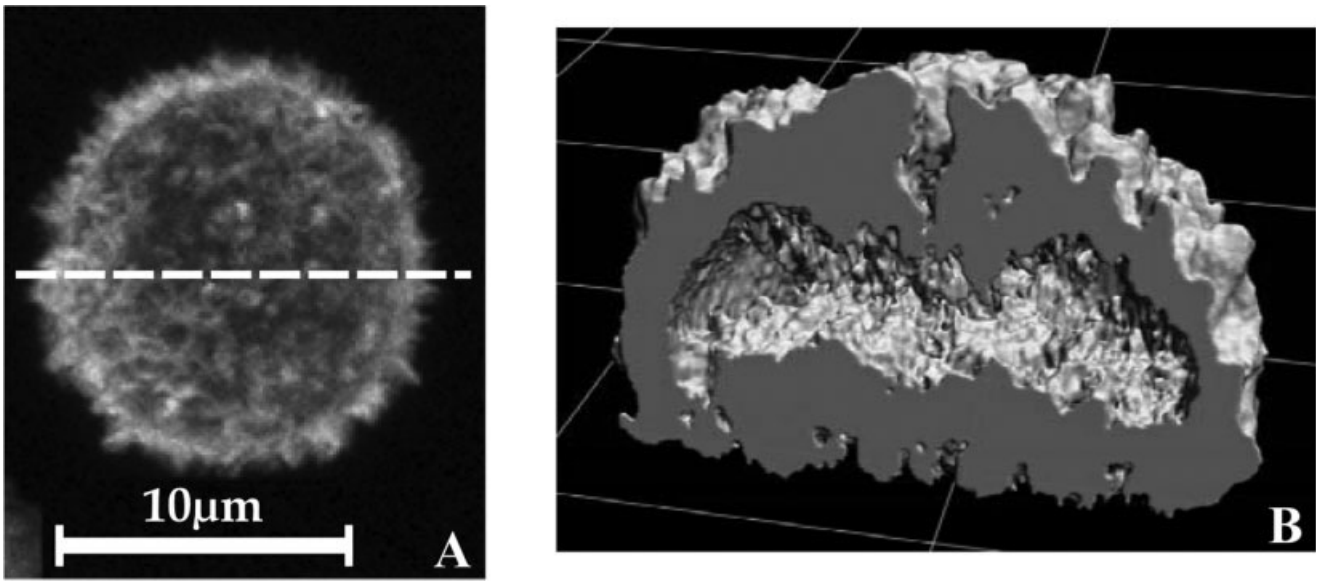

Fig. 3. Spatial reconstruction of F-Actin structure of AMs adherent on glass substrate. In A: View of cumulative confocal microscopic images (z-stack) of the actin cytoskeleton of AM. Staining of F-actin cytoskeleton was performed with rhodamine-phalloidin. In B: cross-sectional view of 3D reconstruction of the actin cytoskeleton structure of a macrophage following the vertical plane defined by the dotted line shown in A (see Materials and Methods). This 3D-reconstruction view is obtained from Z-stack images issued from confocal microscopy with ×100 objective (same in A). Each square is 10 μm.

Characterization of Cytoskeletal Structure and Shape of AMs Cultured on Different Substrates

Spatial reconstructions of F-actin structure permit qualitative and quantitative estimates of main dimensions in fixed AMs (see Materials and Methods). A confocal cumulative image of a typical F-actin structure of an adherent AM with rounded and symmetrical shape is presented in Fig. 3A and the corresponding view of the reconstructed spatial F-actin structure throughout a vertical section is presented in Fig. 3B. These results reveal that the actin cytoskeleton in AMs is essentially cortical and resemble a thick submembranous actin mantle (thickness: 1 to 4 μm) surrounding the entire cell with no evidence of stress fibers or F-actin bundles.

To examine in more details the AMs actin structure for the different substrate studied, we have considered the density of actin structure in 6 μm-thick cell slices from the basal cell face (see Figs. 4A, 4B, 4E, 4F, 4I, 4J, 4M, and 4N). Side views of fluorescence intensity cumulated in between the two vertical planes (dotted lines in Figs. 4A, 4B, 4E, 4F, 4I, 4J, 4M, and 4N) are shown in Figs. 4C, 4D, 4G, 4H, 4K, 4L, 4O, and 4P. These partial

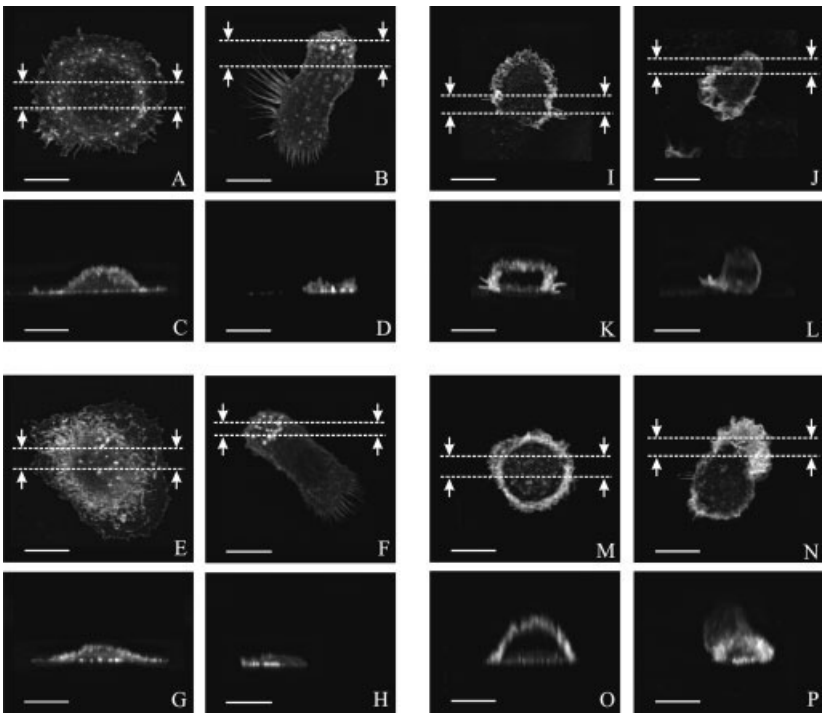

Fig. 4. F-Actin structure of adherent macrophages. Microscopic images of the F-actin cytoskeleton in the neighborhood of basal plane (slices of 6 μm-thick representing about 25 images from the lowest acquired confocal image) of alveolar macrophages with (A, C, E, G, I, K, M, O) and without (B, D, F, H, J, L, N, P) antero-posterior polarization of the structure. Macrophages adhere onto (1) a non-coated (A, B, C, D) or a type I collagen-coated glass substrate (E, F, G, H), (2) alveolar epithelial cell monolayer (I, J, K, L), (3) Flexible polyacrylamide gel substrate (M, N, O, P). These 3D-reconstructions were obtained from Z-stack images obtained by confocal microscopy with a ×100 objective. Staining of F-actin was performed with rhodamine–phalloidin. Images A, B, E, F, I, J, M, N are the views from the top of the culture and images C, D, G. H, K, L, O, P are cross-sectional views from the side between two parallel planes indicated by arrows. These images reveal the presence of podosome-like structures of F-actin near the basal face of macrophages for almost all substrates tested (see Discussion).

reconstructions of AMs F-actin structures are shown (in Fig. 4) for the different substrate studied, i.e., (i) the non coated glass substrate in Figs. 4A–4D, (ii) type I collagen-coated glass (Figs. 4E–4H), (iii) the soft (Figs. 4M and 4O) and/or stiff (Figs. 4N and 4P) polyacrylamide gel substrates (Figs. 4M–4P) and (iv) the epithelial cell substrate (Figs. 4I–4L) within which one can distinguish the two typical antero-posterior cell polarity shapes: symmetrical (see Figs. 4A, 4E, 4I, and 4M) and asymmetrical (see Figs. 4B, 4F, 4J, and 4N). Noteworthy, for all the substrates studied and the various cell polarity shapes, actin structure did not exhibit stress-fibres in these adherent AMs.

Using F-actin reconstructions at the lowest F-actin density, (i.e., lowest detectable fluorescence intensity of F-actin corresponding to the submembranous F-actin structure), we have reconstructed in Fig. 5 the entire F-actin structure of the AMs partially shown in Fig. 4 above. Reconstructed F-actin structures are then characterized by top views and side views for the following substrate properties: (i) rigid glass, i.e., E_{Sglass}: 70 MPa, (see Figs. 5A–5D for uncoated substrate and Figs. 5E and 5F for type I collagen coated substrate), (ii) soft monolayer of adherent epithelial cells, i.e., $Es_{cell} = 0.1$ kPa, (see Figs. 5I–5L), and (iii) two moderately stiff gels with two different values of stiffness, i.e., $Es_{gel} = 40$ kPa (see Figs. 5M and 5O) and 160 kPa (see Figs. 5N and 5P). Reconstructions in Fig. 5 qualitatively show that AM shape is flattened in case of rigid substrates while shape of AMs appear rounded when they adhere on the softer substrates (i.e., for both the moderately stiff gels and the type II alveolar epithelial cell monolayer). Note that AMs adherent on rigid substrates are able to develop numerous long cellular extensions composed of actin structure such as filipodia. By contrast, AMs adherent on physiological cell monolayer substrates do not develop such a type of long actin extension (Figs. 5I and 5J) but rather develop actin microprojections which uniformly cover the AM surfaces (Fig. 5I).

Still concerning these results, it should be also noted that in spite of the heterogeneity of the population of AMs issued from broncho-alveolar lavages (see Materials and Methods), the AM shapes could be partitioned into two basic categories: the symmetrical F-actin shapes (see A, E, I, M in Figs. 4 and 5) and the asymmetrical F-actin shapes (see B, F, J, N in Figs. 4 and 5) which were observed for every types of substrates. Note that in the

Fig. 5. Top and side views of F-actin structures of AMs adhering on substrates of different stiffness. All views show 3D reconstructions of the actin cytoskeleton structure in alveolar macrophages with (A, C, E, G, I, K, M, O) and without (B, D, F, H, J, L, N, P) antero-posterior polarization. Macrophages adhere onto (1) a non-coated (A, B, C, D) or a type I collagen-coated glass substrates (E, F, G, H) (2) alveolar epithelial cell monolayer (I, J, K, L) (3) Flexible polyacrylamide gel substrate (M, N, O, P). These 3D reconstructions were obtained from Z-stack images issued by confocal microscopy using ×100 objective. Staining of F-actin was performed with rhodamine phalloidin. Images A, B, E, F, I, J, M, N are the views from the top of the culture and images C, D, G, H, K, L, O, P are the views from the side indicated by arrows in A. Size of each square: 10 μm.

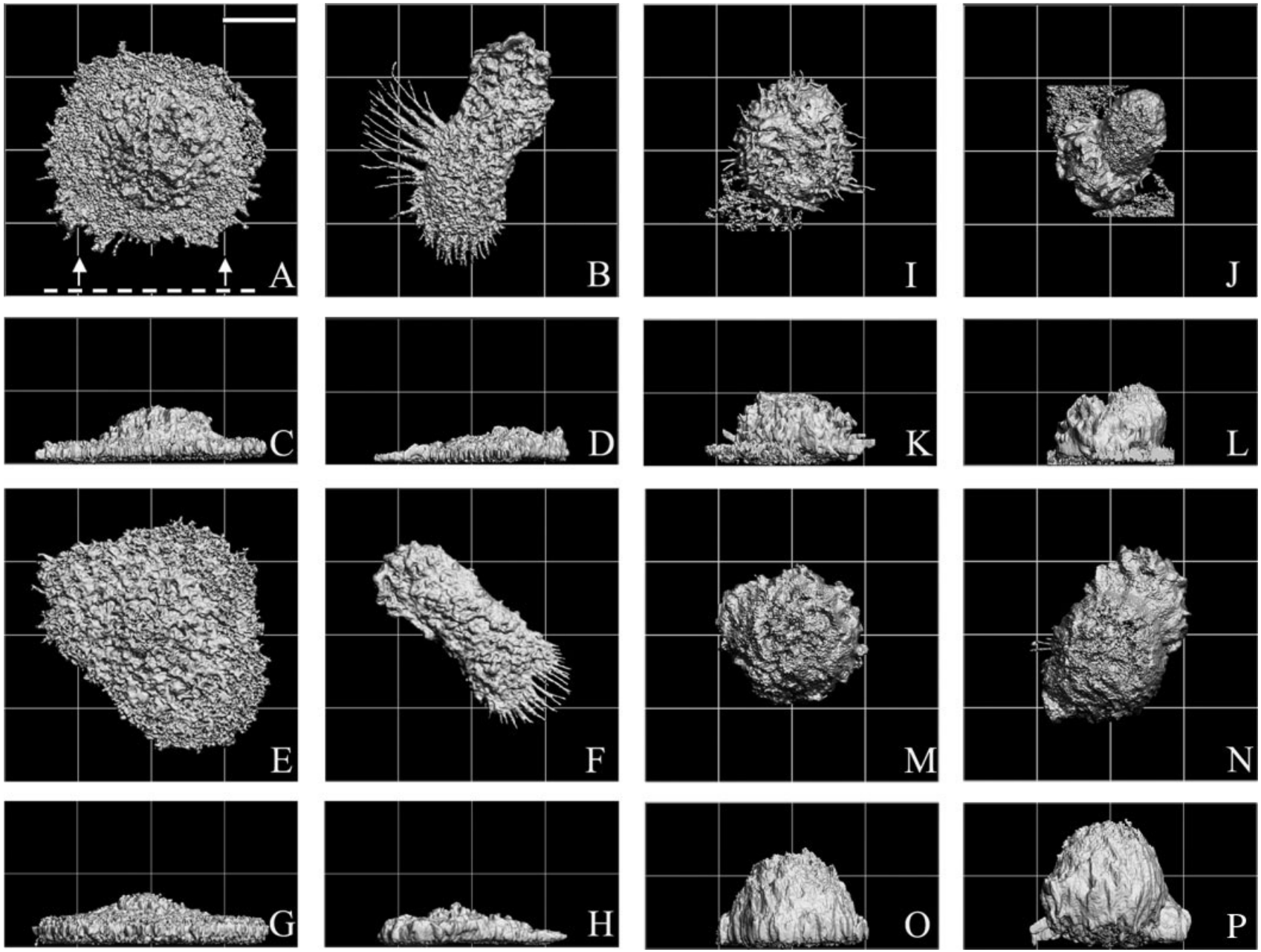

Figure 5.

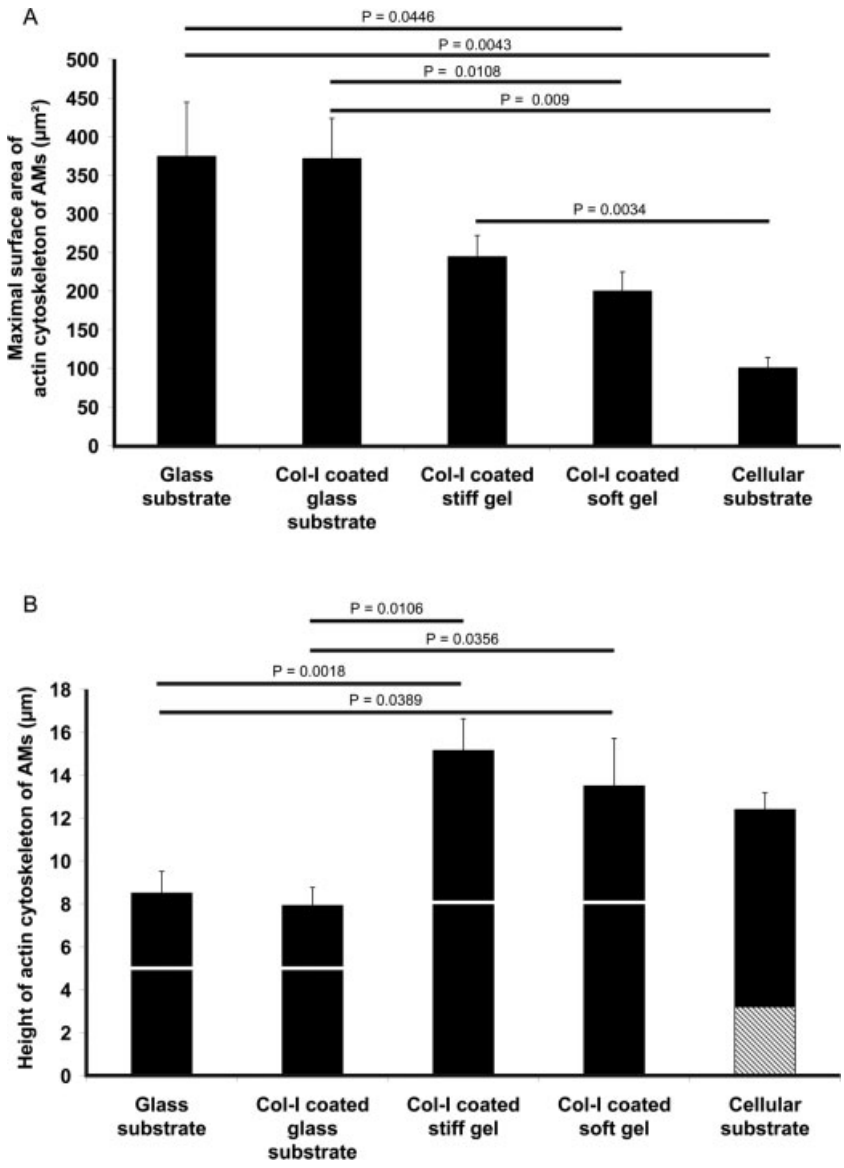

Fig. 6. Maximal surface area and height of F-actin structures in fixed alveolar macrophages adherent on different substrates. In A: Maximum surface area (in μm^2) and in B: maximal height (in µm) of the reconstructed actin cytoskeleton structure for rat alveolar macrophages adhering on (1) Glass substrate (type I collagen-coated or non-coated) (2) Polyacrylamide gel substrate (soft or stiff) (3) alveolar epithelial cell monolayer. Values are mean ± s.e.m. The statistical test used was the Mann–Whitney test ($P < 0.05$). The hatched part illustrates the uncertainty in the determination of the height of respectively the macrophage and the underlying alveolar epithelial cell structure. Indeed, both the actin CSK structures of alveolar macrophage and the alveolar epithelial cells were indifferently stained by rhodamine–phalloidin. We can guess that the height of actin CSK of alveolar macrophages is between 9.5 µm and 12.3 µm. The white lines in the columns B indicate the mean height of alveolar macrophage structures for the various substrates tested.

present culture conditions, the number of AMs with symmetrical shape is about twice the number of cells with asymmetrical shapes. Beyond this antero-posterior shape analysis, the important result to emphasize is that the proportion of flat and rounded AM shapes depends on the type of underlying substrate, namely flattened AM shapes were largely predominant in rigid substrates, (i.e., more than 80% in coated and 65% in uncoated substrates) while rounded shapes were predominantly observed in cell and gel substrates, (i.e., more than 90%). These percentages are calculated by reference to an overall number of cells in the range 600–1000, depending on the type of substrate studied.

To quantify the substrate-dependent changes in AM shape, we calculated, from F-actin reconstructions, the maximal surface area (near the basal plane) and the maximal (and mean) height. The results are ordered for the decreasing values of substrate stiffness (from 70 MPa down to 0.1 kPa). These results are shown in Fig. 6A for the maximal surface area and in Fig. 6B for maximal height. Results clearly show that maximal surface area decreases significantly as substrate stiffness decreases from glass to cell. An opposite tendency is observed for the maximal height of AMs which tends to increase as substrate stiffness decreases. Note that maximal height of the F-actin structure of AMs on cellular substrate was determined but with some uncertainty (see hatched area in right column of Fig 6B) because lack of detectable difference in F-actin density between the apical F-actin face of epithelial cells and the basal face of F-actin structure in AMs. Mean AM height was readily calculated for glass substrate treated with type I collagen

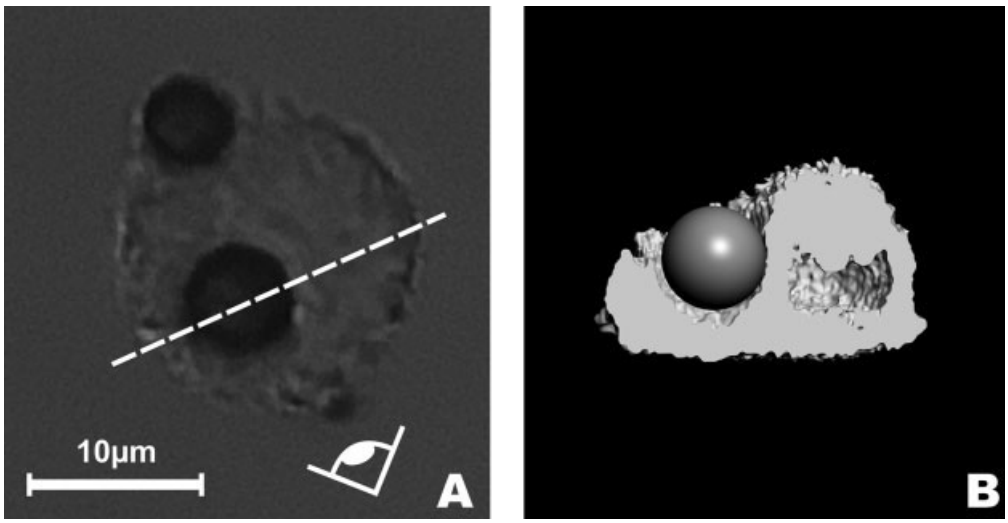

Fig. 7. F-Actin structure of macrophages with immersed RGD-coated beads. In A : Light microscopy view of beads coated with RGD peptide and attached via integrins to the F-actin structure. Note that two beads are attached to this macrophage. This photo was taken with a ×100 objective. In B : cross-sectional view of a 3D-reconstruction of the actin cytoskeleton structure of a macrophage cut by a vertical plane crossing one of the two beads as shown by the dotted line in A. Note that beads are largely immersed in the cytoplasm (half-angle of bead immersion around 100°) and in close contact with the actin structure. This 3D reconstruction was obtained from Z-stack images obtained by confocal microscopy of the cell shown in A.

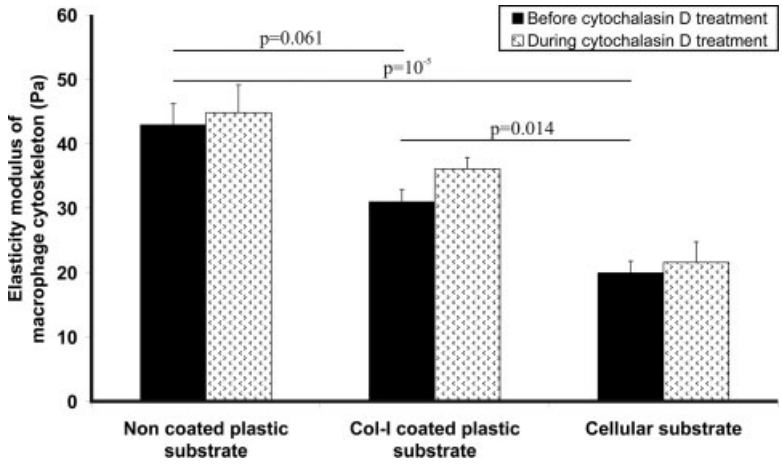

Fig. 8. Elasticity modulus of living alveolar macrophages measured by MTC. Elasticity modulus (in Pa) measured by Magnetic Twisting Cytometry (see Materials and Methods) in macrophages adherent to three different substrates, i.e., successively a non-coated plastic rigid plastic substrate, a type I collagen coated rigid plastic substrate, a type II alveolar epithelial cell monolayer soft substrate. In full dark: control values; discontinuous symbols: after 11 min of F-actin depolymerizing treatment with cytochalasin D. Values are mean ± s.e.m. Each value is the mean of three independent measurements. The statistical test used here is the Anova test. Values of elasticity modulus in macrophages are significantly different between substrates but surprisingly not affected by cytochalasin D treatment (see Results).

or untreated, (i.e., $h_m = 5$ µm) and for the two gel substrates tested, (i.e., $h_m = 8$ µm) (shown in Fig 6B). Note however that there is a lack of significant change in AM spreading area and maximal (or mean) AM height when values of substrate stiffness are not sufficiently different such as (i) between type I collagen coated and non-coated glass substrates (Figs. 6A and 6B), or (ii) between the stiff and the soft flexible polyacrylamide gel substrates tested. These results suggest that the differences in substrate stiffness which lead to changes in AM shape correspond to Young modulus changes greater than three orders of magnitude. Noteworthy, this adaptation of AM actin structure to substrate stiffness does not imply the development of actin stress fibres.

Characterization of Stiffness of AMs Cultured on Different Substrates

The F-actin reconstruction method in the neighborhood of magnetic beads has been first used to assess both the bead attachment to F-actin as well as to determine the half-angle of bead immersion in the AM cytoplasm. An example of F-actin reconstruction is illustrated in Fig. 7 which is similar to Fig. 3 except that two magnetic beads are attached. The vertical section performed on the spatial reconstruction (Fig. 7B) following the axis (shown in Fig. 7A) reveals the large bead engulfment typically observed in AMs as well as the close attachment between F-actin structure and bead surface, the contact surface being well represented by an half-angle of bead immersion of 108°±31° (estimated over 10 beads).

The values of AM elasticity modulus shown in Fig. 8 were obtained in AMs adherent on two different substrates: (i) uncoated and coated with type I collagen plastic substrates (Young modulus: ~3 MPa), and (ii) on a monolayer of alveolar epithelial cells (0.1 kPa), and for two conditions: a control condition (i.e., before cytochalasin D treatment) and during a depolymerizing treatment (i.e., after 11 min of cytochalasin D treatment). As indicated in Materials and Methods, the values reported in Fig. 8 are obtained from apparent stiffness values corrected by a factor which depends on the actual half-angle of bead immersion in AMs, (i.e.,~100°). The results exhibit a statistically significant effect of the substrate stiffness on AM stiffness. More precisely, the mean value (±SEM) of CSK elasticity modulus of AMs adhering on monolayer of alveolar epithelial cells, (i.e., 20 ± 3.3 Pa) appears significantly lower than that obtained on rigid substrates whether they are coated with type I collagen, (i.e., 31 ± 1.8 Pa) or uncoated, (i.e., 43 ± 1.9 Pa). These results show that both adhesive and elasticity properties of underlying substrate affect the AM stiffness but to a limited extent since an increase in substrate stiffness by as much as seven orders of magnitude results in an adhesion-modulated increase in AMs stiffness of +55% for coated substrate and of 115% for uncoated substrate. Surprisingly, this substrate-dependent stiffness of AMs is not affected by actin depolymerization treatment with cytochalasin D. Note that due to the artifact on MTC signal created by the beads that would deposite on the gels (see Materials and Methods), we were not able to measure the stiffness of AMs adhering on gels in the present experimental conditions.

Numerical Model of Macrophage–Substrate Mechanical Interaction

Numerical results shown in Fig. 9 provide an estimate of the "apparent" elasticity modulus sensed by the bead, E_{app}, relatively to the actual "cell" modulus, E_{cell}, (i) as a function of half-angle of bead immersion varying from 15° to 180°. (ii) as a function of cell height (varying from 4 to 11 μm), for soft, intermediate and rigid substrate and a constant angle $\alpha = 130°$ (Fig. 9B).

Curves plotted in Fig. 9A show how half-angle of bead immersion affect the correcting factor E_{app}/E_{cell}. It is interesting to note that E_{app}/E_{cell} is markedly dependent on α but it remains the same whether the tested cell layer is continuous (confluent layer of epithelial cells [Ohayon et al., 2004]) or discontinuous (isolated AMs as in the present study). Curves in Fig. 9B show that the substrate stiffness-dependence of E_{app}/E_{cell} is reinforced in the low range of cell height, i.e., the closer the bead from the substrate, the higher the contribution of the substrate on the bead rotation as pointed out in previous numerical studies [Mijailovich et al., 2002; Ohayon et al., 2004; Ohayon and Tracqui, 2005]. For instance, when the mean cell height of AMs decreases from 8 μm (case of cell substrate) to a value of 5 μm (case of glass substrate), the influence of the substrate stiffness on the measured "apparent" AM stiffness is increased. Then, when the deformation of the basal surface of the cell is limited by an enhanced substrate stiffness, the bead rotation may be limited by a factor which depends on substrate Young's modulus and on the distance between the bead and the substrate. For mechanical reasons, the numerical model predicts a reduction in bead rotation by 20%, i.e., a 20%-increase in AMs Young modulus, from thick AMs adhering on soft substrates to thin AMs on rigid substrate, eventhough this shape transformation pertains to the biological response of AMs, as explained below.

DISCUSSION

AMs are rapidly motile cells which play a central role in the defense of the respiratory apparatus [Brain, 1992]. Due to the wide variety of alveolar micro-environmental conditions which characterize the normal and diseased lungs, AMs are supposed to encounter alveolar walls having a wide variety of mechanical properties as well as largely remodeled extracellular matrix. Reasons are discussed in a specific paragraph below. These factors could influence AM functions. To the best of our knowledge, we present in this study the first results enlightening the sensitivity of macrophages to substrate mechanical and adhesive properties. Noteworthy, the present evaluation of AMs sensitivity is performed based on a new cellular model in which AMs are studied in identical culture conditions. As a matter of fact, the wide majority of AMs (see Results) maintains a symmetrical actin shape without front-rear polarization. This is notably due to the absence of chemo-attractant which guaranteed no chemical activation of AMs in our experimental conditions. On the other hand, we purposely cultured AMs on substrates of quite different stiffnesses, ranging from highly rigid glass substrate to the supple epithelial cell monolayer substrate, thus covering the presumed wide variety of normal and pathological substrate conditions.

Specificity of AMs In Terms of Cytoskeleton Structure and Prestress

From a structural point of view, it has already been shown by Jones et al. that macrophages do not possess stress fibers but have very fine actin cables within the cytoplasm, running parallel to the plasma membrane and around the nucleus [Jones et al., 1998]. Present results

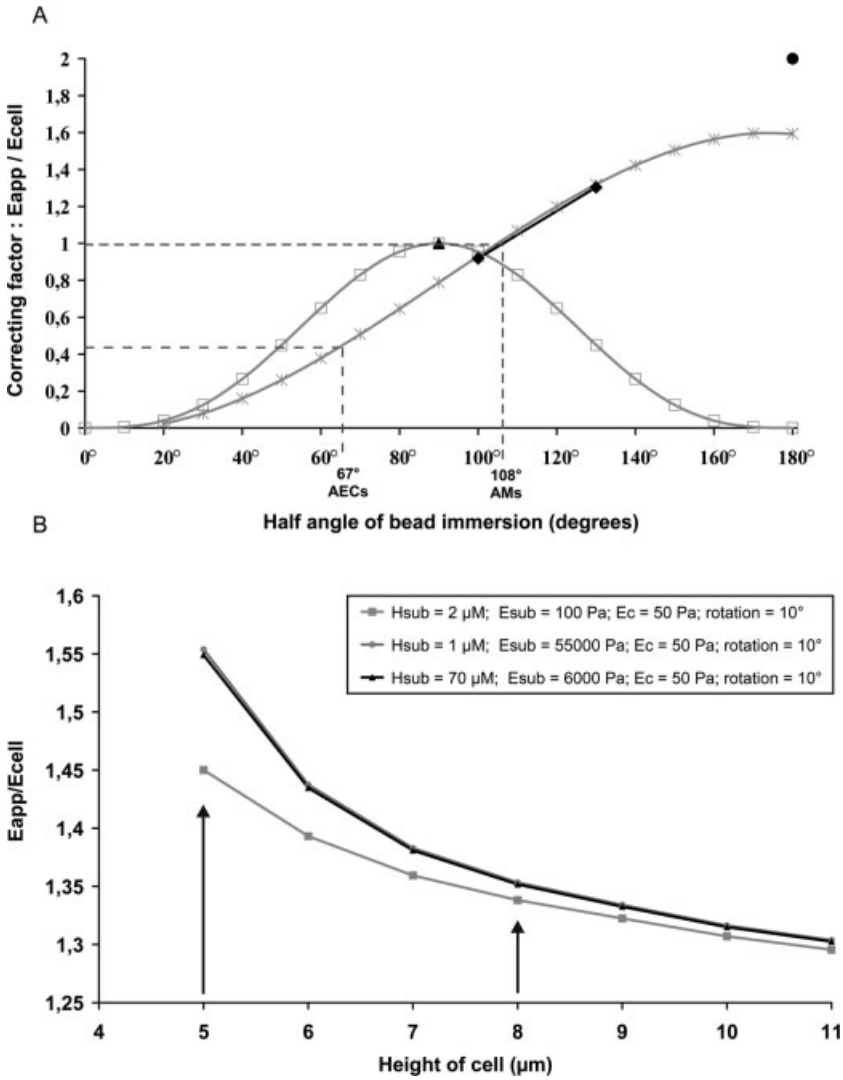

Fig. 9. Numerical estimate of E_{app}/E_{cell} as a function of half-immersion angle and cell height (linear elasticity assumption). $E_{app}/E_{cell} \leq 1$ (respectively ≥ 1) means that measured apparent stiffness underestimates (respectively over-estimates) the actual cell stiffness. In (A): The correcting factor (E_{app}/E_{cell}) is plotted versus the half-angle of bead immersion α assuming a 20 µm-cell-depth (infinite depth) for different assumptions of the numerical model: -symbols ◆ and continuous black line: isolated cells regularly distributed, case of the present AMs study, -symbols × and grey line: monolayer of confluent cells on rigid substrate, case studied by Ohayon and Tracqui (2005), For comparison, we plotted the approximated analytical solution in $\sin^3\alpha$ (symbol □ and grey bell-shaped curve) proposed by Laurent et al., (2002b) which provides a satisfactorily curve fitting in the low α-range, as well as the complete analytical solutions for half-immersed bead (symbol: ▲) and for fully-immersed beads ($\alpha = 180^\circ$, symbol: ●). The difference between the numerical solution and the complete analytical solution at $\alpha = 180^\circ$ is due to differences in geometrical conditions: full-immersion in semi-infinite medium for the numerical solution, full-immersion in an infinite medium for the analytical solution. Note that the difference in half-angle of bead immersion between Alveolar Epithelial Cells (AECs), i.e., α=67°, and Alveolar Macrophages (AMs), i.e., α=108°, lead to a large difference in correcting factor. In (B): The correcting factor (E_{app}/E_{cell}) is plotted versus cell heights. This graph represents the variations in (E_{app}/E_{cell}) measured for increasing values of macrophage height in the range 5 µm–11 µm, a significant 130°-half angle of bead immersion and three values of the couple: substrate height (Hsub)-Young modulus (Esub) (2 µm, 0.1 kPa); (1µm, 55 kPa); (70 µm, 6 kPa), a constant bead rotation of 10° and a fixed macrophage stiffness (Ec) : 50 Pa. The two vertical arrows correspond to the mean height of F-actin structures on rigid glass and gel substrates (see Fig. 6). The increase in E_{app}/E_{cell} as cell height decreases is basically due to the decrease in the distance between the bead bottom and the substrate already described in the literature [Mijailovich et al., 2002; Ohayon and Tracqui, 2005] but importantly reveals an enhanced effect of the substrate stiffness.

shown in Fig. 4 extend these results to alveolar macrophages and reveal that the lack in stress fibers in our AMs is found for the quite different substrate properties studied. A related finding is the lack of cytochalasin D effect on measured AMs stiffness for all substrates tested. Since disruption of F-actin cytoskeleton in AMs does not affect their stiffness, one may expect a low contribution of F-actin to AMs stiffness. Noteworthy, struc-

tural results corroborate mechanical results. AM totally differ from most of commonly cultured adherent cells which are known to generate stress-fibers and accordingly exhibit a high sensitivity to depolymerizing drugs [Wang et al., 1993; Laurent et al., 2002a, 2003; Smith et al., 2005;]. We have previously shown in a culture of epithelial bronchial cells that the highly polymerized stress fibres network structured throughout day 1 to day 4 after seeding, was responsible for the observed increase in cell stiffness which may be seen as an estimate of the actinic contribution to the cell prestress [Doornaert et al., 2003].

Present results suggest that AMs have a negligible level of internal tension at least at the scale at which coated beads (i.e., 4.5 μm in diameter) sense the cell. Noteworthy, the lack of cytochalasin D effect has already been found in previous studies on macrophages. For instance, in a mouse monocyte AM cell line which was phagocyting twistable magnetic beads, AM stiffness was found unaffected by cytochalasin D [Moller et al., 2000; Möller et al., 2001]. Combining Traction Force Microscopy and MTC, Wang et al. have found a positive relationships between cell stiffness and cell prestress [Wang et al., 2002] but this has been obtained in contractile adherent cells which is not the case for the wide majority of our AMs (see Results). The Wang et al.'s study suggests that AMs should generate some prestress during their migration, an assumption which could not be verified with the techniques used in the present study. Indeed, to migrate or perform phagocytosis, AMs most likely generate an internal stress but only locally, e.g., using the actomyosin machinery present in the very local podosome adhesive structures. A recent study has revealed that myosin II-dependent adherent actin microdomains were sensitive to mechanical properties of the environment [Collin et al., 2006]. The local prestress generated in podosomes could not be sensed by the beads, most likely due to the lack of long tensed stress fibers in AMs. In our cellular model, 3D-reconstructions of F-actin structure in the region comprising the interface between the AM and the substrate (Figs. 4A–4L) revealed the presence of these podosomes-like punctuate structures of dense F-actin for all substrates tested. As shown in previous studies [Evans et al., 2003], we found that these punctuate F-actin adhesive structures are observed in lamelipodia of our migrating AMs with polarity shape (Figs. 4B, 4F, 4J, and 4N), and could also be localized in a central part of AMs of any shape (Figs. 4A, 4E, 4I, and 4M). Also, it has been shown [Tanaka et al., 1993] that contractile proteins were concentrated within the protrusions of the ventral cell surface in transformed cells, which are cell-adhesive structures with high motility. Consistently with the lack of cytochalasin D effect found in our AMs, it has been suggested that podosome structural proteins protect short F-actin filaments from depolymerization [DeFife et al., 1999].

Specificity of AMs In Terms of Sensitivity to Substrate Properties

Besides the structural specificity of AM structure described above, the present study brings a series of new information about the AM's sensitivity to substrate properties.

The first important finding concerns the changes in cell shape with substrate stiffness which reveals a sensitivity of AMs to substrate stiffness alterations (see Fig. 4). Using a signalization process which remains to be fully identified, AMs are able to adapt and profoundly modify their shape to the extent that substrate Young modulus is sufficiently modified. As a matter of fact, shape of AMs was totally modified between rigid substrates and soft substrates (i.e., gels and/or cell monolayer) while AM shape remained rounded between stiff and soft gels and even between gels and cell substrates. In the two latter cases, substrates varied their Young Modulus by no more than two or three orders of magnitudes. Noteworthy, AM stiffness measurements show that the mechano-sensitivity of AMs occurs at negligible level of actinic internal tension seen at cell-scale. Note that taking into account the bead size (i.e., 4.5 μm in diameter) and the cell size (i.e., 10–30 μm wide and 5–15 μm high in Fig. 5), that scale of prestress evaluation is closer from the cell scale than any molecular scale. Thus the mechanism used by AMs to probe and respond to their physical environment does not resemble to that previously described for low motile cells. Hence, results obtained in AMs cannot be explained by previous results such as those obtained in smooth muscle cells and endothelial cells [Wang et al., 1993, 2002; Hu et al., 2004, 2005], in fibroblasts [Bausch et al., 1998; Dembo and Wang, 1999; Munevar et al., 2001], in myocytes [Griffin et al., 2004]. Indeed, in these tissue cells, cell prestress is central for mechanosensing and is responsible for cell adaptation to mechanical environment. Present results raise an intriguing question about the mechanosensitive pathways used by AMs to probe their environment since AMs have no tensed cell-scale structure. This point is discussed in the next paragraph.

The second important finding is that stiffness of living AMs is dependent on substrate stiffness. Using the numerical model presented in Materiels and Methods, we have quantified the effect of substrate properties on cell stiffness sensed by the bead. It appears that a rigid substrate imposes a non deformable boundary condition at the basal surface of the AM, which in turn results in an increase in the AM stiffness measured by the bead, the smaller the distance below the bead, the stronger the

substrate stiffness effect. The predicted contribution of substrate stiffness to the AM stiffness (i.e., around 20%) is consistent with experimental results presented in Fig. 8, although slightly underestimating the stiffness increase (i.e., roughly 55% from cell monolayer to glass substrates). Thus, the stiffening effect measured in AMs can likely be understood on the basis of the change in basal cell boundary conditions revealed by the flattening process of AMs, but we cannot exclude a complementary effect such as partial cytoskeleton remodeling, presently not taken into account by the simplified model. Moreover, considering the over simplifications of the model (e.g., in terms of material homogeneity and continuity), the present numerical model likely predicts minimally the changes associated to alterations in boundary conditions.

The third finding concerns the sensitivity of AMs to adhesive properties of the substrate. Results show that AM stiffness is increased from coated to uncoated rigid substrates. These results suggest an adhesion-dependent mechanism capable to enhance the substrate contribution to AM stiffness which is described in a paragraph below.

Specificity of AMs In Terms of Mechanotransduction

AMs are sensitive to substrate properties but they markedly differ from tissue cells in terms of structure and internal tension. Thus, one may question the mechanotransduction pathways used in the context of such a low cellular internal tension.

As a matter of fact, the concept of mechanotransduction is classically used to describe signaling in low motile but highly tensed tissue cells, which are also highly polymerized actin structured cells [Ingber, 1991; Forgacs, 1995; Yamada, 1997; Galbraith and Sheetz, 1998; Geiger and Bershadsky, 2002; Chiquet et al., 2003]. By means of focal adhesion, adhesion forces can stimulate the development of focal contacts [Riveline et al., 2001], while the size of mature focal contacts reversibly increases or decreases as a function of the applied force [Geiger and Bershadsky, 2001]. Molecular interactions between cell and substrate are primarily mediated by integrins, which have been thought to act as strain-gauges triggering signaling pathways involving specific proteins linking cytoskeletal elements, (e.g., MAPK and NF-κB) [Choquet et al., 1997]. Thus, in low motility, firmly adherent and stress-fibre-structured cells, mechano-transduction is possible because the cytoskeleton maintains a sufficient level of cell prestress, such that the stiffer (or tenser) is the cytoskeleton, the more sensitive to external stress is the cell surface which then acts as a strain gauge mechanism [Chiquet et al., 2003]. Note however that adhesion onto soft surfaces mainly supports the development of relatively small, transient, dot-like or fibrillar adhesions that are involved in cell motility and matrix reorganization, respectively [Pelham and Wang, 1997].

Compare to tissue cells, the substrate sensitivity of highly motile cells such as macrophages has been much less studied. Macrophages have been shown to adhere by means of short-lived punctuate adhesion structures notably podosome adhesive structures, which are formed by a diffuse membrane domain of integrins and associated proteins (e.g., vinculin and talin) surrounding a dense actin core [Destaing et al., 2003]. Podosomes therefore clearly differ from other F-actin rich structures such as focal adhesions (also called focal contacts) which characterize adhesion of low motile cells. The core of podosomes is the site of dynamic actin remodeling regulated by WASP and Arp2/3 complex molecules known to be nucleators of actin filaments [Linder et al., 1999; Jones, 2000; Linder and Aepfelbacher, 2003]. Furthermore, the core seems to be surrounded by a cloud of G-actin and to a lesser extent F-actin [Destaing et al., 2003], which might serve as a source of assembly-competent actin for podosome turnover. The present data strongly suggest that podosomes-like adhesive structures presently found in the reconstructed F-actin structure (see Fig. 4), would constitute the mechanosensors in our highly motile AM cells. This suggests that mechanosensitivity of AMs would likely be exacerbated when AMs adopt a migratory phenotype, i.e., lose their symmetrical shape and exhibit a front-rear polarity shape.

It remains remarkable that mechanotransduction however occurs in the context where a wide majority of AMs are mostly symmetrical and without cell shape polarity. To better understand how mechanotransduction could take place in the context of such a low internal tension, it would certainly be useful to investigate the role of other CSK filaments (e.g., microtubules and intermediate filaments) in terms of their contribution to such a process. But investigation of the role of non actinic CSK elements is beyond the scope of the present study. A potentially relevant aspect with microtubules is their reported association with podosomes, being in some cases, in direct contact with them [Linder et al., 2000]. Moreover, their contribution in terms of stabilization and phagocytosis has already been reported [Damiani and Colombo, 2003]. As already discussed above, literature and present results obtained in macrophages suggest that adhesive sites differ structurally and functionally between on the one hand the low tensed macrophages and on the other hand the tissue tensed cells. Tissue cells exhibit stress fibres and focal adhesion sites and thus a periodic distribution of protein-based contractile structures such as myosin or tropomyosin normally exists along stress fibers. In AMs, the presence of contractile apparatus in podosomes [Tanaka et al., 1993] is consistent with

the idea that prestress and migration forces could be generated through the podosomes structures (see above). Another difference concerns the regulation mechanisms which control life time and functions of adhesion sites. Indeed, force-regulation at focal adhesion sites is static and controlled by their size which grows reversibly as force increases [Geiger and Bershadsky, 2001], while force regulation of nascent adhesion sites to which podosomes resemble is highly dynamic and thereby controlled by substrate mechanical properties [Bruinsma, 2005; Collin et al., 2006]. At last, force regulation of immature (i.e., nascent) adhesion sites matches the exerted forces to the stiffness of the substrate [Choquet et al., 1997; Pelham and Wang, 1997]. Noteworthy, our AMs results reveal sensitivity to substrate stiffness which is consistent with the concept of dynamic regulation of nascent adhesion sites.

Validity of the Present Approach

We discuss below the rationale and limits of the present approach considering successively (i) the variety of alveolar wall stiffness in normal and injured lungs, (ii) the applicability of the MTC method to the measurement of AM stiffness and (iii) the contribution of adhesive properties to the stiffness sensitivity of AMs.

Variety of Alveolar Wall Stiffness in Normal and Diseased Lungs. Recent in vitro studies dedicated to the mechanical properties of alveolar epithelial cells (A549) submitted to either cellular stretching through substrate deformation [Trepat et al., 2004], or proinflammatory stimuli (e.g., using thrombin) [Trepat et al., 2005], have shown that epithelial cell stiffness was significantly increased in both cases (i.e., respectively up to 64% and 200%). This stiffening process was associated to a profound reorganization of the actin-cytoskeleton in these alveolar epithelial cells stimulated by mechanical/environmental conditions mimicking that encountered in the fibrotic lung. Repeated stretch of amplitudes up to 50% could even induce cell death in rat primary alveolar epithelial type II cells suggesting that if the forces generated during ventilation exceed certain limits, alveolar epithelial destruction occurs [Tschumperlin and Margulies, 1999]. Thus, in acute lung injury, the normal acinar architecture is initially destroyed and progressively replaced by thick layers of fibrotic tissue, leading to dramatic increase in lung tissue stiffness as the content in collagen fiber, which exponentially increases with the severity of lung injury, increases [Rocco et al., 2001]. Incidentally, the emphysematous lung is also characterized by an increase in collagen content but wall stiffness is smaller than in healthy lungs [Ito et al., 2005] leading to reduction in collagen failure strength and ultimately breakdown of alveolar wall network [Kononov et al., 2001]. Young's modulus of type I collagen has been estimated to be in the range 3–9 GPa for molecules [Sasaki and Odajima, 1996] and 0.5–5 MPa for the highly complexe collagen arrangements called collagen fibrils [Silver et al., 2002]. Incidentally, these values fit the upper range of substrate stiffness values tested in the present study. Collagen is the most important load-bearing element within alveolar duct and wall, its role is thought to be predominant for biomechanical properties of lung parenchyma both in normal and diseased lungs. By comparison, non collagenic elements such as elastic fibers, proteoglycans, interstitial cells and surfactant most likely play a role but to a lesser extent [Suki et al., 2005]. Noteworthy, surfactant generates prestress on alveolar ducts walls and, by distorting their geometry, alters the elastic properties of the connective tissues [Stamenovic, 1990]. However, for small deformations (e.g., normal breathing) surface film viscoelasticity would be less important than lung tissue viscoelasticity [Schurch et al., 1992]. Because numerous mechanical and biomechanical factors contribute to collagen production and assembly, one may expect a wide variability in collagen fiber properties, content and distribution within the alveolar ducts and alveolar walls of a given lung. Using a model of alveolar wall deformation which combines the distributed nature of collagen properties and the limiting effects of proteoglycan matrix, the average Young Modulus of the normal alveolar wall was estimated to be around 5 kPa [Cavalcante et al., 2005], i.e., a stiffness value located right in between the cellular and the gel substrates used in the present study. The elements above enlighten the interest of testing a wide range of alveolar substrate stiffness such as done in the present study.

Applicability of the MTC Method to the Measurement of AM Stiffness. The MTC method based on bead rotation measurement, so improved as described above by the bead immersion model (see Materials and Methods), appeared to be particularly adapted to the large bead rotations (i.e., 25–47° in AMs) and to the large bead engulfment ($\alpha = 108^\circ \pm 30^\circ$) encountered in AMs.

Concerning the results on mechanical sensitivity of AMs, a critical aspect concerns the MTC method presently used to quantify cell mechanical properties and cell prestress. The major drawback raised by Fabry et al. in 1999 concerns the effect of non-attached beads that freely rotate during magnetic torque application which are responsible for an artefactual response leading to strongly underestimate the actual cell stiffness modulus [Fabry et al., 1999]. We like to mention concerning that free rotating bead artifact that this phenomenon happens to be important but only in the low range of applied torque, i.e., typically below 10 Pa (see Fig. 5 in [Fabry et al., 1999]). Since we presently used torques above

400 pN × μm (i.e., ~10 Pa of stress), present experiments were actually performed above the range of torque where these artifacts become critically important. We have recently shown from epithelial cells that the MTC method based on bead rotation measurements, not only tolerates a certain degree of bead heterogeneity inherent to the cellular heterogeneity, but advantageously homogenizes non-necessarily constant cellular medium properties. This is due to the large number of beads involved which act as many local probes randomly distributed throughout the cell culture [Ohayon et al., 2004]. Concerning the MTC method presently used, it should be emphasized that the isolated character of macrophages does not modify the correction coefficient established for a cell monolayer (see Fig. 9A in Results and [Ohayon et al., 2004; Ohayon and Tracqui, 2005]) as far as an appropriate half-angle of bead immersion is estimated [Fodil et al., 2003] .

Using the combined theoretical/experimental correction described above, MTC data converge towards the values obtained by other - non MTC - techniques. Indeed, for the same A549 epithelial cells cultured on glass substrates, we presently find E_{cell}=0.1 kPa with MTC, Laurent et al. found E_{cell}=0.125 kPa with lazer tweezers [Laurent et al. 2002b], whereas Alcaraz et al. found E_{cell}=0.159 kPa with Atomic Force Microscopy [Alcaraz et al., 2003]. This gives some confidence in the values presently found for AMs. Interestingly enough, for the same glass substrate and in the present experimental culture conditions, MTC results show that AMs elasticity modulus, i.e., 0.045 kPa, is about half the values found in epithelial cells. The residual discrepancies between methods have been discussed in previous papers and includes heterogeneity between cells and structures [Laurent et al., 2003], differences between types and magnitude of local stresses applied [Ohayon et al., 2004].

Contribution of Adhesive Properties to the Stiffness Sensitivity of AMs. Macrophage adhesion is the result of molecular interactions that have been characterized and quantified for each substrate studied. Specific inhibition of adhesion to the various substrates tested (see Fig. 2) showed that AMs systematically interact via β_2-subunit integrins which is in agreement with results previously reported by Albert et al. [Albert et al., 1992; Ross, 2000]. These authors showed that adding monoclonal antibody directed against β_2-subunit integrins decreased adhesion of human macrophages onto TNFα-stimulated human cells (A549).

To explain the remaining part of AM adhesion after eliminating interactions via β_2-subunit integrins (see Fig. 2), (i.e., for all non-specific adhesion substrates tested: non-coated glass and cellular monolayer substrates), several additional adhesion mechanisms can be postulated. Tomita et al. [Tomita and Ishikawa, 1992] identified two 12 and 14 kDa glass-adherent proteins purposely named "attachmin" considered to be responsible for non-specific adhesion of mouse peritoneal macrophages while Ono et al. [Ono et al., 1993] showed that actin cytoskeleton is closely associated with these glass-adherent proteins. We postulate that non-specific adhesion proteins tend to reinforce AM adhesion, in parallel with β_2-subunit integrins. Thus, the enhanced AM stiffness observed for the non-coated stiff substrate could be attributed to a stronger AM-substrate interaction.

In the context of AM adhesion to physiological substrates, the natural linkage with α_M/β_2 integrins at the basal surface of AMs occurs via ICAM-1 mechanoreceptors expressed at the apical surface of alveolar epithelial cells [Paine et al., 2002; Planus et al., 2005]. However, the residual adhesion secondary to anti-β_2 on the physiological substrate (see Fig. 2) might be attributed to receptors other than ICAM-1 receptors, as other receptors or even integrins could also contribute to AM adhesion on alveolar epithelial cells [Albert et al., 1992]. In assessing the shape and stiffness of AMs adhering specifically via β_2 subunits, we observed that non-specific adhesion conditions, (i.e., non-coated glass substrate and cell monolayer substrate) lead to either a stiffened and flattened AM or a softened and rounded AM. This suggests that non-specific adhesion may lead to a variety of outcomes. In parallel, numerical simulations suggest a contribution of substrate stiffness to the measured AM stiffness. The difference in adhesive sensitivity of AMs observed between type I collagen-coated and non-coated rigid substrates suggests that adhesive conditions might modulate the measured stiffness and could thus better transmit the substrate stiffness effect.

CONCLUSIONS

In conclusion, the present study reveals that AMs exhibit, as most of tissue cells, a sensitivity to microenvironment, except that AM mechanotransduction could not be mediated by cell-scale internal tension given to characterize tissue cells. AMs respond to important changes in substrate stiffness, e.g., from soft (cell monolayer or gels) to rigid substrates by (i) flattening their F-actin shape without generating stress fibers, (ii) increasing their stiffness without increasing their internal tension "seen" by twisted beads. This increase in AM stiffness depends on whether substrate adhesion is specific or not. On the whole, the mechanical and chemical sensitivity of AMs appears to be mediated by highly dynamic nascent adhesion sites well represented by podosomes whose structure and function differ from the mature focal contacts largely encountered in tissue cells. More-

over, under the present experimental conditions, most of AMs keep a symmetrical and rounded shape when cultured on physiological substrate while, in tissue cells, rounded shapes often lead to apoptotic fate. The flattened shape of AMs encountered when cultured on rigid substrates could be seen as the specific response of AMs to the phagocytosis of infinitely large rigid particles.

ACKNOWLEDGMENTS

Authors gratefully thank Jacques Ohayon for help in elaborating the numerical model and Christophe Tourain for performing AFM measurements on gels of polyacrylamide. We also gratefully thank Région d'Ile-de-France for Financial support of the AFM equipment acquired by University Paris XII.

REFERENCES

Albert RK, Embree LJ, McFeely JE, Hickstein DD. 1992. Expression and function of beta 2 integrins on alveolar macrophages from human and nonhuman primates. Am J Respir Cell Mol Biol 7(2):182–189.

Alcaraz J, Buscemi L, Grabulosa M, Trepat X, Fabry B, Farre R, Navajas D. 2003. Microrheology of human lung epithelial cells measured by atomic force microscopy. Biophys J 84(3):2071–2079.

Bachofen H, Schurch S. 2001. Alveolar surface forces and lung architecture. Comp Biochem Physiol A Mol Integr Physiol 129(1): 183–193.

Balaban NQ, Schwarz US, Riveline D, Goichberg P, Tzur G, Sabanay I, Mahalu D, Safran S, Bershadsky A, Addadi L, Geiger B. 2001. Force and focal adhesion assembly: A close relationship studied using elastic micropatterned substrates. Nat Cell Biol 3(5): 466–472.

Bausch AR, Ziemann F, Boulbitch AA, Jacobson K, Sackmann E. 1998. Local measurements of viscoelastic parameters of adherent cell surfaces by magnetic bead microrheometry. Biophys J 75(4): 2038–2049.

Beningo KA, Dembo M, Kaverina I, Small JV, Wang YL. 2001. Nascent focal adhesions are responsible for the generation of strong propulsive forces in migrating fibroblasts. J Cell Biol 153(4):881–888.

Beningo KA, Wang YL. 2002. Flexible substrata for the detection of cellular traction forces. Trends Cell Biol 12(2):79–84.

Ben-Ze'ev A, Farmer SR, Penman S. 1988. Cell–cell and cell–matrix interactions differentially regulate the expression of hepatic and cytoskeletal genes in primary cultures of rat hepocytes. Proc Natl Acad USA 85:2161–2165.

Bissell MJ, Barcellos-Hoff MH. 1987. The influence of extracellular matrix on gene expression: Is structure the message? J Cell Sci Suppl 8:327–343.

Brain JD. 1992. Mechanisms, measurement, and significance of lung macrophage function. Environ Health Perspect 97:5–10.

Bruinsma RF. 2005. Theory of force regulation by nascent adhesion sites. Biophys J 89(1):87–94.

Cavalcante FS, Ito S, Brewer K, Sakai H, Alencar AM, Almeida MP, Andrade JS, Jr, Majumdar A, Ingenito EP, Suki B. 2005. Mechanical interactions between collagen and proteoglycans: Implications for the stability of lung tissue. J Appl Physiol 98(2):672–679.

Chiquet M, Renedo AS, Huber F, Fluck M. 2003. How do fibroblasts translate mechanical signals into changes in extracellular matrix production? Matrix Biol 22(1):73–80.

Choquet D, Felsenfeld DP, Sheetz MP. 1997. Extracellular Matrix Rigidity Causes Strengthening of Integrin-Cytoskeleton Linkages. Cell 88:39–48.

Chrzanowska-Wodnicka M, Burridge K. 1996. Rho-stimulated contractility drives the formation of stress fibers and focal adhesions. J Cell Biol 133:1403–1415.

Clerici C, Friedlander G, Amiel C. 1992. Impairment of sodium-coupled uptakes by hydrogen peroxide in alveolar type II cells: Protective effect of d-alpha-tocopherol. Am J Physiol 262(5 Pt 1): L542–L548.

Collin O, Tracqui P, Stephanou A, Usson Y, Clement-Lacroix J, Planus E. 2006 Spatio-temporal dynamic of actin-rich adhesion microdomain: Influence of substrate flexibility. J Cell Sci 119.09, in press.

Damiani MT, Colombo MI. 2003. Microfilaments and microtubules regulate recycling from phagosomes. Exp Cell Res 289(1): 152–161.

DeFife KM, Jenney CR, Colton E, Anderson JM. 1999. Cytoskeletal and adhesive structural polarizations accompany IL-13-induced human macrophage fusion. J Histochem Cytochem 47(1):65–74.

Dembo M, Wang YL. 1999. Stresses at the cell-to-substrate interface during locomotion of fibroblasts. Biophys J 76(4):2307–2316.

Destaing O, Saltel F, Geminard JC, Jurdic P, Bard F. 2003. Podosomes display actin turnover and dynamic self-organization in osteoclasts expressing actin-green fluorescent protein. Mol Biol Cell 14(2):407–416.

Discher DE, Janmey P, Wang YL. 2005. Tissue cells feel and respond to the stiffness of their substrate. Science 310(5751):1139–1143.

Doornaert B, Leblond V, Planus E, Galiacy S, Laurent VM, Gras G, Isabey D, Lafuma C. 2003. Time course of actin cytoskeleton stiffness and matrix adhesion molecules in human bronchial epithelial cell cultures. Exp Cell Res 287(2):199–208.

Engler A, Bacakova L, Newman C, Hategan A, Griffin M, Discher D. 2004. Substrate compliance versus ligand density in cell on gel responses. Biophys J 86(1 Pt 1):617–628.

Evans JG, Correia I, Krasavina O, Watson N, Matsudaira P. 2003. Macrophage podosomes assemble at the leading lamella by growth and fragmentation. J Cell Biol 161(4):697–705.

Fabry B, Maksym G, Hubmayr R, Butler J, Fredberg J. 1999. Implications of heterogeneous bead behavior on cell mechanical properties measured with magnetic twisting cytometry. J Magn Magn Mater 194:120–125.

Fodil R, Laurent VM, Planus E, Isabey D. 2003. Characterization of cytoskeleton mechanical properties and 3D-actin structure in twisted living adherent cells. Biorheology 40(1,2,3):241–245.

Folkman J, Moscona A. 1978. Role of Cell Shape in Growth Control. Nature 273:345–349.

Forgacs G. 1995. On the possible role of cytoskeletal filamentous networks in intracellular signaling: An approach based on percolation. J Cell Sci 108:2131–2143.

Galbraith CG, Sheetz MP. 1998. Forces on adhesive contacts affect cell function. Curr Opin Cell Biol 10:566–571.

Geiger B, Bershadsky A. 2001. Assembly and mechanosensory function of focal contacts. Curr Opin Cell Biol 13(5):584–592.

Geiger B, Bershadsky A. 2002. Exploring the neighborhood: Adhesion-coupled cell mechanosensors. Cell 110(2):139–142.

Griffin MA, Engler AJ, Barber TA, Healy KE, Sweeney HL, Discher DE. 2004. Patterning, prestress, and peeling dynamics of myocytes. Biophys J 86(2):1209–1222.

Hu S, Chen J, Wang N. 2004. Cell spreading controls balance of prestress by microtubules and extracellular matrix. Front Biosci 9:2177–2182.

Hu S, Chen J, Butler JP, Wang N. 2005. Prestress mediates force propagation into the nucleus. Biochem Biophys Res Commun 329(2):423–428.

Ingber D. 1991. Integrins as mechanochemical transducers. Curr Opin Cell Biol 3:841–848.

Ito S, Ingenito EP, Brewer KK, Black LD, Parameswaran H, Lutchen KR, Suki B. 2005. Mechanics, nonlinearity, and failure strength of lung tissue in a mouse model of emphysema: Possible role of collagen remodeling. J Appl Physiol 98(2):503–511.

Jones GE. 2000. Cellular signaling in macrophage migration and chemotaxis [In Process Citation]. J Leukoc Biol 68(5):593–602.

Jones GE, Allen WE, Ridley AJ. 1998. The Rho GTPases in macrophage motility and chemotaxis. Cell Adhes Commun 6(2–3):237–245.

Kononov S, Brewer K, Sakai H, Cavalcante FS, Sabayanagam CR, Ingenito EP, Suki B. 2001. Roles of mechanical forces and collagen failure in the development of elastase-induced emphysema. Am J Respir Crit Care Med 164(10 Pt 1):1920–1926.

Laplante C, Lemaire I. 1990. Interactions between alveolar macrophage subpopulations modulate their migratory function. Am J Pathol 136(1):199–206.

Laurent VM, Cañadas P, Fodil R, Planus E, Asnacios A, Wendling S, Isabey D. 2002a. Tensegrity behaviour of cortical and cytosolic cytoskeletal components in twisted living adherent cells. Acta Biotheor 50(4):331–356.

Laurent VM, Hénon S, Planus E, Fodil R, Balland M, Isabey D, Gallet F. 2002b. Assessment of mechanical properties of adherent living cells by bead micromanipulation: Comparison of magnetic twisting cytometry vs optical tweezers. J Biomech Eng 124(4): 408–421.

Laurent VM, Fodil R, Cañadas P, Féréol S, Louis B, Planus E, Isabey D. 2003. Partitioning of cortical and deep cytoskeleton responses from transient magnetic bead twisting. Ann Biomed Eng 31(10):1263–1278.

Linder S, Aepfelbacher M. 2003. Podosomes: Adhesion hot-spots of invasive cells. Trends Cell Biol 13(7):376–385.

Linder S, Nelson D, Weiss M, Aepfelbacher M. 1999. Wiskott-Aldrich syndrome protein regulates podosomes in primary human macrophages. Proc Natl Acad Sci USA 96(17):9648–9653.

Linder S, Hufner K, Wintergerst U, Aepfelbacher M. 2000. Microtubule-dependent formation of podosomal adhesion structures in primary human macrophages. J Cell Sci 113:4165–4176.

Lo CM, Wang HB, Dembo M, Wang YL. 2000. Cell movement is guided by the rigidity of the substrate. Biophys J 79(1):144–152.

Mijailovich SM, Kojic M, Zivkovic M, Fabry B, Fredberg JJ. 2002. A finite element model of cell deformation during magnetic bead twisting. J Appl Physiol 93(4):1429–1436.

Miyamoto S, Akiyama SK, Yamada KM. 1995. Synergistic roles for receptor occupancy and aggregation in integrin transmembrane function. Science 267(5199):883–885.

Moller W, Nemoto I, Matsuzaki T, Hofer T, Heyder J. 2000. Magnetic phagosome motion in J774A. 1 macrophages: Influence of cytoskeletal drugs. Biophys J 79(2):720–730.

Möller W, Kreyling WG, Kohlhäufl M, Häussingger K, Heyder J. 2001. Macrophage functions measured by magnetic microparticles in vivo and in vitro. J Magn Magn Mater 225:218–225.

Mooney DJ, Langer R, Ingber DE. 1995. Cytoskeletal filament assembly and the control of cell spreading and function by extracellular matrix. J Cell Sci 108 (Pt 6):2311–2320.

Munevar S, Wang YL, Dembo M. 2001. Distinct roles of frontal and rear cell-substrate adhesions in fibroblast migration. Mol Biol Cell 12(12):3947–3954.

Ohayon J, Tracqui P. 2005. Computation of adherent cell elasticity for critical cell-bead geometry in magnetic twisting experiments. Ann Biomed Eng 33(2):131–141.

Ohayon J, Tracqui P, Fodil R, Féréol S, Laurent VM, Planus E, Isabey D. 2004. Analysis of nonlinear responses of adherent epithelial cells probed by magnetic bead twisting: A finite element model based on a homogenization approach. J Biomech Eng 126(6): 685–698.

Ono M, Murakami T, Tomita M, Ishikawa H. 1993. Association of the actin cytoskeleton with glass-adherent proteins in mouse peritoneal macrophages. Biol Cell 77(2):219–230.

Paine R, III, Morris SB, Jin H, Baleeiro CE, Wilcoxen SE. 2002. ICAM-1 facilitates alveolar macrophage phagocytic activity through effects on migration over the AEC surface. Am J Physiol Lung Cell Mol Physiol 283(1):L180–L187.

Pelham RJ, Jr, Wang Y. 1997. Cell locomotion and focal adhesions are regulated by substrate flexibility. Proc Natl Acad Sci USA 94(25):13661–13665.

Planus E, Galiacy S, Féréol S, Fodil R, Laurent VM, d'Ortho M-P, Isabey D. 2005 Apical rigidity of an epithelial cell monolayer evaluated by Magnetic Twisting Cytometry: ICAM-1 versus Integrin linkages to F-actin structure. Clin Hemorheol and Microcirc 33(3):277–291.

Planus E, Galiacy S, Matthay M, Laurent V, Gavrilovic J, Murphy G, Clérici C, Isabey D, Lafuma C, d'Ortho MP. 1999. Role of collagenase in mediating in vitro alveolar epithelial wound repair. J Cell Sci 112 (Pt 2):243–252.

Pugin J, Dunn I, Jolliet P, Tassaux D, Magnenat JL, Nicod LP, Chevrolet JC. 1998. Activation of human macrophages by mechanical ventilation in vitro. Am J Physiol 275(6 Pt 1):L1040–L1050.

Riveline D, Zamir E, Balaban NQ, Schwarz US, Ishizaki T, Narumiya S, Kam Z, Geiger B, Bershadsky AD. 2001. Focal contacts as mechanosensors: Externally applied local mechanical force induces growth of focal contacts by an mDia1-dependent and ROCK-independent mechanism. J Cell Biol 153(6):1175–1186.

Rocco PR, Negri EM, Kurtz PM, Vasconcellos FP, Silva GH, Capelozzi VL, Romero PV, Zin WA. 2001. Lung tissue mechanics and extracellular matrix remodeling in acute lung injury. Am J Respir Crit Care Med 164(6):1067–1071.

Ross GD. 2000. Regulation of the adhesion versus cytotoxic functions of the Mac-1/CR3/alphaMbeta2-integrin glycoprotein. Crit Rev Immunol 20(3):197–222.

Rossman MD, Cassizzi AM, Daniele RP. 1980. Adherence and morphology of guinea pig alveolar macrophages: Effect of N-formyl methionyl peptides. Infect Immun 29(3):1185–1189.

Sasaki N, Odajima S. 1996. Stress-strain curve and Young's modulus of a collagen molecule as determined by the X-ray diffraction technique. J Biomech 29(5):655–658.

Schurch S, Bachofen H, Goerke J, Green F. 1992. Surface properties of rat pulmonary surfactant studied with the captive bubble method: Adsorption, hysteresis, stability. Biochim Biophys Acta 1103(1):127–136.

Sheetz MP, Felsenfeld DP, Galbraith CG. 1998. Cell migration: Regulation of force on extracellular-matrix-integrin complexes. Trends Cell Biol 8(2):51–54.

Silver FH, Horvath I, Foran DJ. 2002. Mechanical implications of the domain structure of fiber-forming collagens: Comparison of the molecular and fibrillar flexibilities of the alpha1-chains found in types I-III collagen. J Theor Biol 216(2): 243–254.

Smith BA, Tolloczko B, Martin JG, Grutter P. 2005. Probing the viscoelastic behavior of cultured airway smooth muscle cells with atomic force microscopy: Stiffening induced by contractile agonist. Biophys J 88(4):2994–3007.

Stamenovic D. 1990. Micromechanical foundations of pulmonary elasticity. Physiol Rev 70(4):1117–1134.

Suki B, Ito S, Stamenovic D, Lutchen KR, Ingenito EP. 2005. Biomechanics of the lung parenchyma: Critical roles of collagen and mechanical forces. J Appl Physiol 98(5):1892–1899.

Tanaka J, Watanabe T, Nakamura N, Sobue K. 1993. Morphological and biochemical analyses of contractile proteins (actin, myosin, caldesmon and tropomyosin) in normal and transformed cells. J Cell Sci 104 (Pt 2):595–606.

Tomita M, Ishikawa H. 1992. Identification of novel adhesion proteins in mouse peritoneal macrophages. Biol Cell 76(1):103–109.

Trepat X, Grabulosa M, Puig F, Maksym GN, Navajas D, Farre R. 2004. Viscoelasticity of human alveolar epithelial cells subjected to stretch. Am J Physiol Lung Cell Mol Physiol 287(5): L1025–L1034.

Trepat X, Grabulosa M, Buscemi L, Rico F, Farre R, Navajas D. 2005. Thrombin and histamine induce stiffening of alveolar epithelial cells. J Appl Physiol 98(4):1567–1574.

Tschumperlin DJ, Margulies SS. 1999. Alveolar epithelial surface area–volume relationship in isolated rat lungs. J Appl Physiol 86(6):2026–2033.

Wang N, Butler JP, Ingber DE. 1993. Mechanotransduction across the cell surface and through the cytoskeleton [see comments]. Science 260(5111):1124–1127.

Wang N, Tolic-Norrelykke IM, Chen J, Mijailovich SM, Butler JP, Fredberg JJ, Stamenovic D. 2002. Cell prestress. I. Stiffness and prestress are closely associated in adherent contractile cells. Am J Physiol Cell Physiol 282(3):C606–C616.

Wang YL, Pelham RJ, Jr. 1998. Preparation of a flexible, porous polyacrylamide substrate for mechanical studies of cultured cells. Methods Enzymol 298:489–496.

Wendling S, Planus E, Laurent V, Barbe L, Mary A, Oddou C, Isabey D. 2000. Role of cellular tone and microenvironmental conditions on cytoskeleton stiffness assessed by tensegrity model. Eur Phys J Appl Phys 9:51–62.

Yamada KM. 1997. Integrin signaling. Matrix Biol 16(4):137–141.

Yeung T, Georges PC, Flanagan LA, Marg B, Ortiz M, Funaki M, Zahir N, Ming W, Weaver V, Janmey PA. 2005. Effects of substrate stiffness on cell morphology, cytoskeletal structure, and adhesion. Cell Motil Cytoskeleton 60(1):24–34.